# Investigation of the generation of high-order harmonics through Bohmian trajectories

Yang Song,[1] Fu-Ming Guo,[1] Su-Yu Li,[1] Ji-Gen Chen,[2,*] Si-Liang Zeng,[3,†] and Yu-Jun Yang[1,‡]

[1]*Institute of Atomic and Molecular Physics, Jilin University, Changchun 130012, China*

[2]*Department of Physics and Materials Engineering, Taizhou University, Taizhou 318000, China*

[3]*Institute of Applied Physics and Computational Mathematics, Beijing 100088, China*

(Received 10 June 2012; published 24 September 2012)

We theoretically investigated the generation progress of high-order harmonics utilizing Bohmian trajectories, which are calculated from the accurate numerical wave function. It is found that the harmonic emission spectrum from atoms in an intense laser field calculated by Bohmian trajectories agrees well with that found by numerically solving the time-dependent Schrödinger equation. Through the analysis of the dynamic behavior of Bohmian trajectories, we investigated the ionization process, the acceleration of the ionized electron in the laser field, and its recollision with the parent ion in the progress. Furthermore, the individual behavior and the coherent contribution of these trajectories to the harmonic emission are discussed.

DOI: 10.1103/PhysRevA.86.033424 PACS number(s): 32.80.Rm, 42.50.Hz

## I. INTRODUCTION

When intense laser pulses interact with atoms and molecules, one can observe the high-order-harmonic generation (HHG) [1]. Driven by the linearly polarized monochromatic laser pulse, a plateau structure for the HHG spectrum exists, and the cutoff energy of the plateau is $I_p + 3.2U_p$, where $I_p$ is the atomic ionization energy, $U_p = {E_0}^2/4\omega^2$ is the pondermotive energy, and $E_0$ and $\omega$ refer to the maximum amplitude and frequency of laser pulse, respectively. Due to the unique plateau structure of the harmonic spectrum, HHG can be utilized to generate soft x-ray source and ultrashort attosecond pulses. Since the first observation of HHG in an experiment at the end of 1980s, HHG has become a hot research topic because of its significant application background [2–4].

For theoretical research of HHG, it is necessary to numerically solve the time-dependent Schrödinger equation (TDSE), which describes the motion of atoms in a laser field. At present, the solution to the TDSE is mainly through the numerical integration scheme, which can accurately describe the dynamic evolution of the system. However, more computational resources are needed, and it is difficult to extract the needed physical information from the numerical results [5–7]. Under this circumstance, classical calculation (CC) [8] and strong-field approximation (SFA) [9] are developed to solve such a process. The CC has the advantage of high computational efficiency, and the physical mechanism during the dynamic process can be well illustrated by analyzing the trajectories of classical particles. However, the quantum coherence and wave-packet dispersion are not considered; therefore, accurate results cannot be obtained. The SFA can analytically solve the time-dependent dipole matrix element, which can be interpreted as the probability amplitude superposition of three dynamic processes: the electronic wave-packet tunneling into the continuous state, oscillating in the laser field, and finally returning to the nuclear zone and interfering with the ground state. Therefore, a lot of information is contained in the SFA scheme, but the contribution of excited states to HHG are not taken into account in this scheme. On the premise that the calculation is accurate, the time-dependent Bohmian trajectories are adopted to describe the dynamic process of the interaction between an intense laser and atoms and molecules so as to clearly illustrate the mechanism of HHG [10–13]. Lai *et al.* [11] calculated the spectrum of harmonic generation according to one Bohmian trajectory, and the propagation effects of HHG are considered. The calculated HHG spectra are in qualitative agreement with the result from TDSE [13].

The dynamic process of electrons cannot be accurately described through only one Bohmian trajectory. In this paper, we select adequate Bohmian trajectories simulating the motion of the electronic wave packet and the HHG process. It is found that the dynamic evolution of the wave packet and the HHG spectrum calculated by adequate Bohmian trajectories are identical to those found by numerically solving the TDSE. According to the information from the trajectories obtained by calculation, the dynamic process of harmonic generation can be well understood.

## II. THEORETICAL METHODS

In order to use the Bohmian trajectories to simulate the HHG process, we need to calculate the probability density distribution of the electronic wave packet. In this paper, a one-dimensional atom model is adopted because, for HHG, one-dimensional and three-dimensional calculational results are qualitatively identical in the linearly polarized incident laser field [14–17]. Under the dipole approximation in the length gauge, the TDSE which describes the interaction between an intense laser and atoms is given by (atomic units are used throughout, unless otherwise stated)

$$i\frac{\partial}{\partial t}\psi(x,t) = \left[-\frac{\partial^2}{2\partial x^2} + V(x) + V_L(x,t)\right]\psi(x,t), \qquad (1)$$

where $V(x)$ is the soft Coulomb potential $V(x) = -q/\sqrt{x^2 + A}$ we adopted, whose parameters are selected as $A = 0.367$ and $Q = 0.561$, and the energies of ground state and first excited state are $E_0 = -0.5$ and $E_1 = -0.125$,

*tz501@yahoo.cn

†zengsiliang@iapcm.ac.cn

‡yangyj@jlu.edu.cn

 

respectively. $V_L(x,t) = E(t)x$ is the interaction between the electron and the laser electric field. The ground-state wave function of the system is acquired by numerically solving the Schrödinger equation, and the initial position of the Bohmian trajectories is calculated by the distribution function $|\psi(x,0)|^2$ of the electronic probability density in the ground state. Once the positions of these particles are determined, the probability density of every trajectory is assumed to be the same, i.e., $1/N_{\rm tra}$, where $N_{\rm tra}$ denotes the number of Bohmian particles chosen. According to Bohmian mechanics [18,19], the motion of Bohmian particles can be solved by the Bohm-Newton equation $\frac{d^2r}{dt^2} = -\nabla(V+Q)$, where $Q = -\frac{1}{2}\frac{\nabla^2 R}{R}$ is the quantum potential and $R$ is the modulus of the wave function. The velocity of a Bohmian particle is

$$v^k(t) = \mathrm{Im}\left[\frac{1}{\psi^k(x,t)}\frac{\partial}{\partial x}\psi^k(x,t)|_{x=x^k(t)}\right] (k = 1,2,\ldots,N_{\rm tra}). \tag{2}$$

Integrating the equation, the position of the Bohmian particle at moment $t$ is obtained: $x^k(t) = x^k(t=0) + \int_0^t v^k(t')dt'$. According to the position and velocity of the Bohmian particle, its kinetic energy and acceleration can be obtained, i.e., $E^k(t) = \frac{1}{2}v^k(t)^2$ and $a^k(t) = dv^k(t)/dt$, respectively. In addition, the force of Bohmian particles can also be obtained through the potential function. Taking the statistical average of $N_{\rm tra}$ particle trajectories as the time-dependent dipole of a whole electron, the high-order-harmonic spectra can be obtained by Fourier transformation of the dipole:

$$\begin{aligned} P(\omega) &= \left|\sum_{k=1}^{N}\tilde{x}^{(k)}(\omega)/N_{\rm tra}\right|^2 \\ &= \left|\frac{1}{N_{\rm tra}(t_f - t_i)}\sum_{k=1}^{N}\int_{t_i}^{t_f} x^{(k)}(t)e^{-i\omega t}dt\right|^2, \end{aligned} \tag{3}$$

which can be expanded as

$$\begin{aligned} P(\omega) = &\sum_{k=1}^{N}\left|\frac{1}{(t_f - t_i)}\int_{t_i}^{t_f}\frac{x^{(k)}(t)}{N_{\rm tra}}e^{-i\omega t}dt\right|^2 \\ &+\sum_{k=1}^{N}\sum_{j=1,j\neq k}^{N}\mathrm{Re}\left[\frac{1}{(t_f - t_i)}\int_{t_i}^{t_f}\frac{x^{(k)}(t)}{N_{\rm tra}}e^{-i\omega t}dt\right. \\ &\left.\times\left(\frac{1}{(t_f - t_i)}\int_{t_i}^{t_f}\frac{x^{(j)}(t)}{N_{\rm tra}}e^{-i\omega t}dt\right)^*\right], \end{aligned} \tag{4}$$

where the first term accounts for noncoherent superposition and the second one refers to interference between Bohmian particles.

## III. RESULTS AND DISCUSSION

As for the dynamic process of an atom in an intense laser field, it can be described either by solving the probability density of the time-dependent wave function or by Bohmian trajectories. According to the information on Bohmian trajectories, a reconstruction of the corresponding electronic probability density can be realized. Figure 1(a) shows the time-dependent evolution of the electronic probability density reconstructed by $N = 20\,000$ Bohmian particles. For comparison, we also

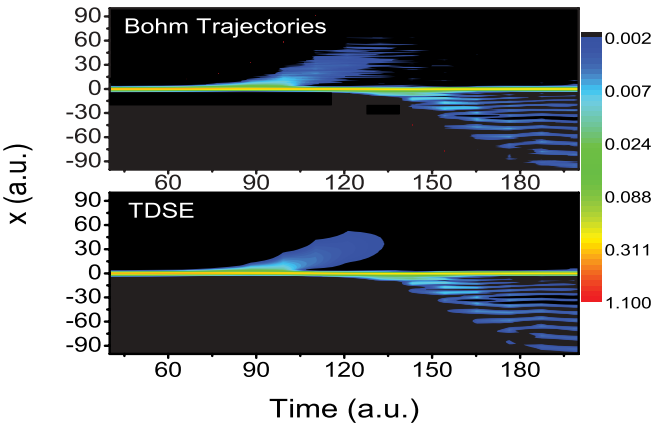


FIG. 1. (Color online) Time-dependent motion of a wave packet reconstructed by Bohmian trajectories and obtained by numerically solving the TDSE.

calculate the evolution of the time-dependent wave packet by solving the TDSE, which is shown in Fig. 1(b). From Fig. 1(b) we see that the results reconstructed by Bohmian trajectories are in good agreement with those obtained by solving the TDSE. This result demonstrates that the motion of the electronic wave packet can be described by Bohmian trajectories accurately. Here, the electric field of the laser pulse is $E(t) = E_0\sin(\omega t)\sin^2(\omega t/\tau)$, maximum amplitude is $E_0 = 0.1$, pulse duration is $\tau = 4$, and wavelength is 800 nm.

By using the Bohmian trajectories, the time-dependent dipole of atoms in an intense laser pulse can be obtained. Figure 2 shows the harmonic spectra simulated by Bohmian trajectories and obtained by numerically solving the TDSE. The dash-dotted blue, dotted green, and dashed red curves correspond to the results from Bohmian particles, the number of which are 500, 5000, and 50 000, respectively. From Fig. 2, one can see that the HHG spectra from Bohmian trajectories from 500 to 50 000 are gradually close to that from numerically solving the TDSE, and when the number of Bohmian trajectories increases to 50 000, its spectrum is almost identical to that obtained by solving the TDSE. These results show that when one utilizes the Bohmian trajectories to simulate the HHG, accurate and convergent harmonic spectra will not be obtained unless the number of Bohmian trajectories is adequate. Here, the Bohmian trajectories are calculated

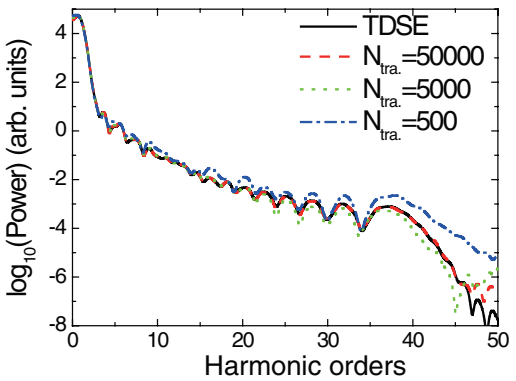


FIG. 2. (Color online) Harmonic spectra obtained by calculating Bohmian trajectories and numerically solving the TDSE.

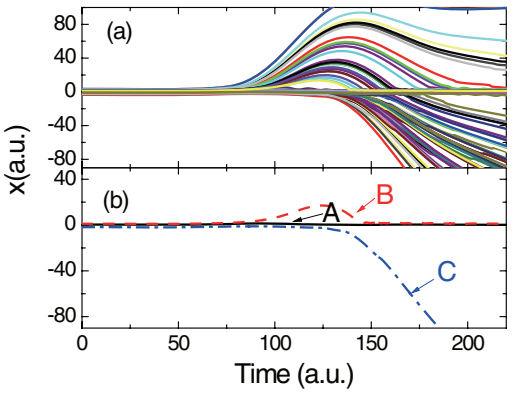


FIG. 3. (Color online) Time-dependent evolution of Bohmian trajectories.

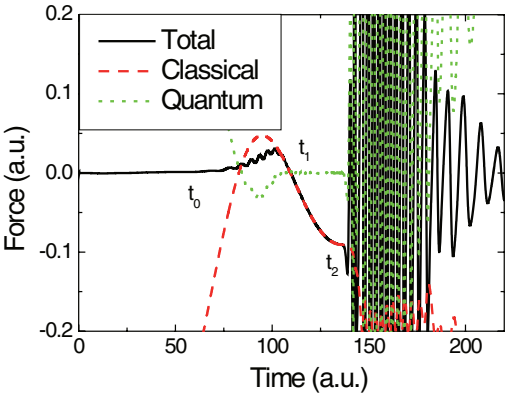


FIG. 4. (Color online) Time-dependent force evolution of Bohmian particle B: the total force (solid black curve), total electric-field force and Coulomb force (dashed red curve), and quantum force (dotted green curve).

from the time-dependent wave function in our calculation. In addition, in order to obtain an accurate result from Bohmian trajectories, we need to choose a large number of trajectories to present the same time-dependent density of trajectories as the density of quantum probability. Thus, the computational cost of the Bohmian trajectory calculation is higher than for the TDSE calculation. However, additional information can be found by using the information from Bohmian trajectories, such as the equivalent definition of classical and quantum chaos [20]. In this paper, we will interpret the physical progress of high-order-harmonic generation by using information from Bohmian trajectories.

The results obtained by numerically solving the TDSE can be accurately reproduced by the time-dependent Bohmian trajectories; more importantly, the physical mechanism can be investigated by analyzing the dynamic behavior of Bohmian trajectories. Figure 3 presents the time-dependent evolution of the Bohmian trajectories of the electron driven by a laser pulse. According to the motion of Bohmian particles, the trajectories of particle motion can be divided into three kinds, and in order to understand the dynamic behavior of each kind of particle, one trajectory selected from each type is also shown in Fig. 3(b).

(1) The first kind of particle shows that the particles are always located in the nuclear zone within the laser pulse duration and do not move with the driving electric field, as shown in Fig. 3(b), curve A (solid black curve). This kind of particle denotes the behavior of a bound electron.

(2) The second kind of particle shows that the particles are accelerated in the positive direction along the $x$ axis, moving away from nuclear zone gradually, and then return to the nuclear zone and are bound again, which is shown in Fig. 3(b), curve B (dashed red curve).

(3) The third kind of particle shows that the particles are bound in the nuclear zone and then are accelerated in the negative direction along the $x$ axis away from the nuclear zone, which is shown in Fig. 3(b), curve C (dash-dotted blue curve).

In order to investigate the HHG mechanism from Bohmian trajectories, we need to analyze their motions. In the following we taking trajectory B; for example, its position, velocity, and acceleration are calculated.

Figure 4 shows the force felt by Bohmian particle B, where the solid black curve is the total force, the dashed red curve refers to the classical force, which includes the electric-field force and the Coulomb force, and the dotted green curve accounts for the quantum force. Figure 5 shows the evolution of the spatial position and velocity of particle B. The dynamic process of particle B can be understood by its position, velocity, and force. One can observe from Fig. 5 that the instantaneous amplitude of the electric field is relatively small when $t < t_0$; therefore, for the particle, the Coulomb force almost balances the quantum force, it is located in the nuclear zone, and its velocity is low. When $t > t_0$, the classical force (the total of Coulomb force and electric-field force) does not balance the quantum force; as a result, the total force is not zero, and its direction is along the positive $x$ axis. Then under the effect of this force, the particle moves from the nuclear zone to the outer space and finally gets rid of the constraint of the nucleus around $t = t_1$. This process corresponds to the so-called tunneling ionization; i.e., the electrons penetrate the potential barrier constituted by the electric potential and the Coulomb potential. However, when the quantum potential is considered, the particle is not affected by the potential barrier, and it will move away from the nuclear zone under the collaborative effect of the electric-field force, the Coulomb force, and the quantum force. Then quantum force tends to be zero as the particle is far away from the nuclear zone; therefore

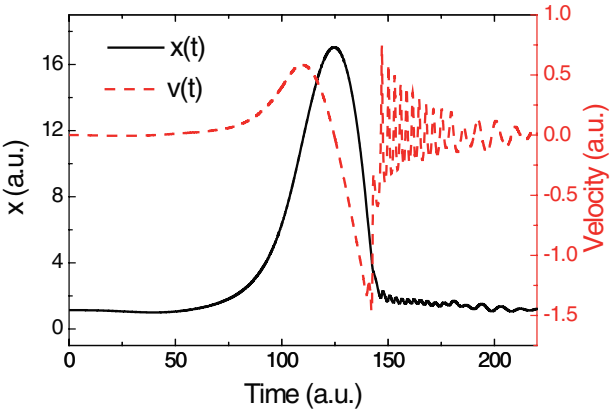


FIG. 5. (Color online) Time-dependent evolution of spatial position (solid black curve) and velocity (dashed red curve).

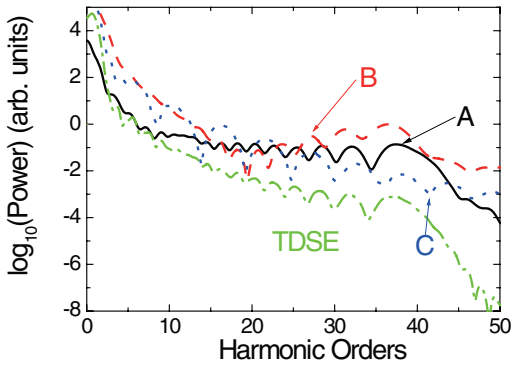


FIG. 6. (Color online) Harmonic spectra of Bohmian particles A, B, and C and that (dash-dotted green curve) obtained by numerically solving the TDSE.

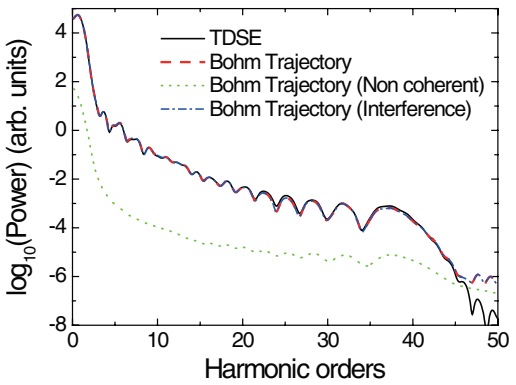


FIG. 7. (Color online) Harmonic spectra obtained with the average of the Bohmian particles' dipole acceleration (dashed red curve), the noncoherent spectrum of the Bohmian particles (dotted green curve), the coherent emission spectrum of the Bohmian particles (dash-dotted blue curve), and the HHG calculated from the TDSE (solid black curve).

the particle is mainly driven by the electric-field force, and when the electric field reverses, it will first decelerate and then accelerated reversely. The particle returns to the nuclear zone at about $t = t_2$, and it is mainly driven by the periodically changed quantum force; therefore the particle has periodic vibration, the amplitude of which decreases gradually. We know the periodic oscillation of the charged particle is accompanied by electromagnetic radiation, and the frequency of radiation is that of the oscillation of the particle; i.e., this process is accompanied by a high-frequency photon emission, whose frequency is 1.9 a.u. (about the 33rd harmonic).

Figure 6 shows the harmonic spectra calculated with the time-dependent dipole of Bohmian particles A, B, and C. For comparison, the HHG spectrum from numerically solving the TDSE is also presented. For particle C, its harmonic spectrum has no clear cutoff. For particle B, there is a strong harmonic generation at the cutoff; however, the oscillating structure of its harmonic is somewhat different from that obtained by numerically solving TDSE. For particle A, its harmonic structure is identical to that obtained by numerically solving the TDSE, and this is in agreement with the numerical results of Lai *et al.* [13]. One can notice that the spectrum of HHG cannot be accurately described by that of a single trajectory; more Bohmian particles need to be considered for an accurate description.

The harmonic generation can be regarded as the collective effect of these Bohmian particles. In order to investigate the coherence of these Bohmian particles, according to Eq. (5), the contribution of the Bohmian particles to the harmonic should be classified into coherent and noncoherent parts. In Fig. 7, the results of the harmonic by numerically solving the TDSE and the harmonic spectrum with Bohmian particles is identical to that from numerically solving the TDSE. Particularly, it can be found from Fig. 7 that the harmonic of the Bohmian trajectories mainly comes from the interference between particles. Therefore, the process of harmonic generation is the coherent superposition of all the Bohmian particles' radiation.

## IV. CONCLUSION

In conclusion, the HHG process of atoms in an intense laser field is investigated by time-dependent Bohmian trajectories. We found that the harmonic spectrum from selecting adequate Bohmian trajectories agrees well with that from numerically solving the TDSE. Through analyzing the dynamic behavior of the Bohmian trajectories, the Bohmian particles describing electrons have the chance to move away from the nuclear zone under the effect of intense laser pulses, the behavior of which is close to classical particles, finally recombining with the parent ion, leading to the photon emission, and the coherence of all Bohmian particles results in the high-order-harmonic generation.

## ACKNOWLEDGMENTS

This work was supported by the National Basic Research Program of China (973 Program) 2013CB922200, the National Natural Science Foundation of China under Grants No. 11274141, No. 11034003, No. 10904006, and No. 11274001, and the Natural Science Foundation of Zhejiang Province under Grant No. Y6110578. We acknowledge the High Performance Computing Center of Jilin University for supercomputer time. Y.-J.Y. would like to acknowledge the warm hospitality of the Institute of Applied Physics and Computational Mathematics during the period when this work was performed.

[1] X. F. Li, A. L' Huiller, M. Merray, and G. Mainfray, Phys. Rev. A **39**, 5751 (1989).

[2] Ch. Spielmann, N. H. Burnett, S. Sartania, R. Koppitsch, M. Schnurer, C. Kan, M. Lenzner, P. Wobrauschek, and F. Krausz, Science **278**, 661 (1997).

[3] P. M. Paul, E. S. Toma, P. Breger, G. Mullot, F. Auge, P. Balcou, H. G. Muller, and P. Agostini, Science **292**, 1689 (2001).

[4] M. Hentschel, R. Kienberger, C. Spielmann, G. A. Reider, N. Milosevic, T. Brabec, P. Corkum, U. Heinzmann, M. Drescher and F. Krausz, Nature (London) **414**, 509 (2001).

[5] J. L. Krause, K. J. Schafer, and K. C. Kulander, Phys. Rev. Lett. **68**, 3535 (1992).
[6] M. Protopapas, C. H. Keitel, and P. L. Knight, Rep. Prog. Phys. **60**, 389 (1997).
[7] K. Burnett, V. C. Reed, and P. L. Knight, J. Phys. B **26**, 561 (1993).
[8] R. Uzdin and N. Moiseyev, Phys. Rev. A **81**, 063405 (2010).
[9] M. Lewenstein, P. Balcou, M. Y. Ivanov, A. L'Huillier, and P. B. Corkum, Phys. Rev. A **49**, 2117 (1994).
[10] P. Botheron and B. Pons, Phys. Rev. A **82**, 021404(R) (2010).
[11] X. Y. Lai, Q. Y. Cai, and M. S. Zhan, New J. Phys. **11**, 113035 (2009).
[12] N. Takemoto and A. Becker, J. Chem. Phys. **134**, 074309 (2011).
[13] Q. Y. Cai, M. S. Zhan, and X. Y. Lai, Chin. Phys. B **19**, 020302 (2010).
[14] J. G. Chen, S. L. Zeng, and Y. J. Yang, Phys. Rev. A **82**, 043401 (2010).
[15] J. G. Chen, Y. J. Yang, S. L. Zeng, and H. Q. Liang, Phys. Rev. A **83**, 023401 (2011).
[16] J. G. Chen, Y. J. Yang, X. P. Yu, L. J. He, and Y. Y. Xu, Acta Phys. Sin. **60**, 053206 (2011).
[17] J. G. Chen, Y. J. Yang, and Y. Chen, Acta Phys. Sin. **60**, 033202 (2011).
[18] R. E. Wyatt, *Quantum Dynamics with Trajectories* (Springer, New York, 2005).
[19] P. Holland, *The Quantum Theory of Motion* (Cambridge University Press, Cambridge, 1993), Chap. 7.
[20] F. H. M. Faisal and U. Schwengelbeck, Phys. Lett. A **207**, 31 (1995).